



Al Mukhtar Journal of Sciences
Vol (28), No. (02), Year (2013) 31-48
Omar Al Mukhtar University, Al Bayda, Libya.
National Library No.: 280/2013/Benghazi

Measurement of 3D Displacement Fields and Deformation Using 3D Laser Scanner and CCD Camera (0-10 mm)

Rahel.G. Rahel¹

¹Mechanical Engineering Department, Faculty of Engineering, Omar Al-Mukhtar University, Tobruk- Libya. Email: Rahelmar@yahoo.fr

DOI: <https://doi.org/10.54172/mjsc.v28i2.157>

Abstract

Many applications dealing with the mechanical behavior of materials require the measurement of displacement fields or deformation fields. For this type of measurement, optical methods have become unavoidable due to their non-intrusive approach, their high spatial resolution, their high sensitivity, the large size of their examined field, and the increasing power of the computers that now allow the processing of huge quantities of data. In this context we have developed a system for measuring 3-D displacement fields using CCD (camera charge digital) and 3D laser scanner. This method allows the measure of the 3-D displacement field using at least two pairs of stereoscopic images of an object corresponding to two states of its deformation (or the processing of a sequence of pairs of images acquired during the deformation). The main topics developed in this study are: the calibration of a camera and a 3D laser scanner, and measuring 3D displacement fields from coupling of camera and 3D laser sensor. The potential application of our method is the characterization of structures, for example, to provide assistance in the development of tools for stamping.

الملخص العربي

العديد من التطبيقات تتعامل مع السلوك الميكانيكي للمواد التي تتطلب مقياس مجال الإزاحة ومجالات التشويه. لهذا النوع من المقياس، الطرق البصرية أصبحت من المستحيل تجنبها بسبب نظرتها الغير تداخلية، قدرتها المكانية العالية، حساسيتها العالية، الحجم الكبير لمجال الفحص، وزيادة قوة الحاسوب الذي يسمح الآن بمعالجة الكميات الضخمة للبيانات. في هذا السياق طورنا نظام لقياس مجالات الإزاحة ثلاثية الأبعاد باستخدام آلة تصوير (كاميرا CCD) وليزر. هذه الطريقة

Received, May 15, 2013; accepted, November 13, 2013

© The Author(s). This open access article is distributed under a CC BY-NC 4.0 license.

تسمح قياس مجال الإزاحة باستخدام على الأقل زوجان رقمية من الصور التجسيمية لجسم متماثل لحالتين لتشويهه (أو معالجة سلسلة من أزواج الصور المكتسبة أثناء التشويه). المواضيع الرئيسية التي طورت في هذه الدراسة هي معايرة الكاميرا وليزر، وقياس مجالات الإزاحة ثلاثي الأبعاد من الأزواج الكاميرا ومحسس الليزر ثلاثي الأبعاد التطبيق المحتمل لطريقتنا هو التمثيل للتركيب، على سبيل المثال، لتزويد المساعدة في تطوير أدوات الختم.

Keywords: *camera calibration, measuring 3-D displacement fields, 3D laser sensor calibration, non- contacting 3-D metrology..*

1. Introduction

Optical methods for measuring displacement are now widely used in mechanical experiments. The main techniques are photoelasticity, geometric moire, moire interferometry, holographic interferometry, speckle interferometry (speckle), the grid method and digital image correlation Frey, P.J. and George, P.L. (1999), CLOUD, G. (1998), Kinsey, L.C. (1993), Sutton, M.A. (1983&1986), Faugeras, OD. And Toscani, G. (1987), Horaud, R. And Monga, O. (1995). Method of digital image correlation (DIC) is probably one of the most commonly used, many applications of DIC method are presented by Horaud, R. (1995) and more specifically for the measurement of displacement fields from 3D stereo coupling and monitoring correlation of pixels in a sequence of images by correlation Garcia, D. (2001), Garcia, D., Orteu, J.J. and Devy, M. (2000), Garcia, D., Orteu, J.J., and Devy, M.(2001).

When only one camera is used, the DIC can give the displacement field only in the planar domain of the observed object. Otherwise using a camera accompanied with a laser sensor 3D, can be measure the displacement field in the 3D surface.

In this study we use the camera and an image correlation method to define the displacement field of a moving object. The coupling of the camera and the 3D scanner allows us to associate the observed displacement field and the 3D surface of the object. The measured displacements are on the 3D surface of the order of 20 mm to 40 mm.

2. Camera calibration and 3D scanner

2.1. Calibration parameters of the camera

The calibration of a camera is to determine the coordinates (u, v) in the image coordinate system (b) from the coordinates (x, y, z) in the coordinate B world. In other words, it consists in solving the following equation:

$$b = M_c(B) \quad (1)$$

To do this, we must first express B in the camera frame, and then calculate the coordinates of (b) in the same spot after a projection. Finally, changes in the b mark image plane for its coordinates (u, v).

2.1.1. Determination of b form

To calculate the coordinates of b in the image plane from point B whose coordinates are expressed in the reference world.

$$\begin{pmatrix} su \\ sv \\ s \end{pmatrix} = \mathbf{M}_C \begin{pmatrix} x \\ y \\ z \\ 1 \end{pmatrix} \quad (2)$$

$$\text{Where } M_C = \begin{pmatrix} m_{11} & m_{12} & m_{13} & m_{14} \\ m_{21} & m_{22} & m_{23} & m_{24} \\ m_{31} & m_{32} & m_{33} & m_{34} \end{pmatrix}$$

In this equation, the coordinates are homogeneous. The homogeneous coordinates of the object point B ($x, y, z, 1$), and those of the pixel b is (su, sv, s). Cartesian coordinates of b are ($su / s, sv / s$). is the perspective projection matrix. Using equation (2), However ,we can write the Cartesian coordinates of an image point as shown in equation (3).

$$\begin{aligned} u &= \frac{m_{11}x + m_{12}y + m_{13}z + m_{14}}{m_{31}x + m_{32}y + m_{33}z + m_{34}} \\ v &= \frac{m_{21}x + m_{22}y + m_{23}z + m_{24}}{m_{31}x + m_{32}y + m_{33}z + m_{34}} \end{aligned} \quad (3)$$

2.1.2. Calculating calibration parameters

The calibration parameters can be obtained from the perspective projection matrix M_C . We apply the method to calculate Faugeras-Toscani M_C (1986, 1987).

The calibration parameters of a camera intrinsic parameters to include a_u, a_v, u_0, v_0 and extrinsic parameters (R) rotation matrix and (T) transition matrix. These parameters can be calculated from the perspective projection matrix M_C . Equation (4) shows how to calculate the calibration parameters from the M_C matrix .

$$\begin{aligned}
 r_3 &= m_3 \\
 u_0 &= m_1.m_3 \\
 v_0 &= m_2.m_3 \\
 a_u &= -\|m_1 \wedge m_3\| \\
 a_v &= \|m_2 \wedge m_3\| \\
 r_1 &= 1/a_u(m_1 - u_0m_3) \\
 r_2 &= 1/a_v(m_2 - v_0m_3) \\
 t_x &= 1/a_u(m_{14} - u_0m_{34}) \\
 t_y &= 1/a_v(m_{24} - v_0m_{34}) \\
 t_z &= m_{34}
 \end{aligned} \tag{4}$$

2.2. Method for 3D laser sensor calibration

The 3D scanner is composed of a sensor and a laser sheet coordinate measuring machine. It helps to have a dense cloud of points with an accuracy of the order of 10 microns. The calibration pattern is used marble cube whose faces are perpendicular. Two checkerboard patterns as were positioned on the faces oriented along the X and Y directions of the machine. Each level of the target is represented by a cloud of points (x, y, z) as shown in Figure 1.

Plane must be perpendicular to the target. The least squares method, is used to calculate the normal vector to each plane, and the intersection of the three planes representing the origin of the coordinate of the target. The origin of the pattern allows us to compute the translation parameters of the transition matrix scanner. three normal vectors (n_1, n_2, n_3) represent the rotation matrix. Then, it is possible to find the transformation matrix between the scanner and the 3D sights.

$$M_s = \begin{pmatrix} R & t \\ 0 & 1 \end{pmatrix} \tag{5}$$

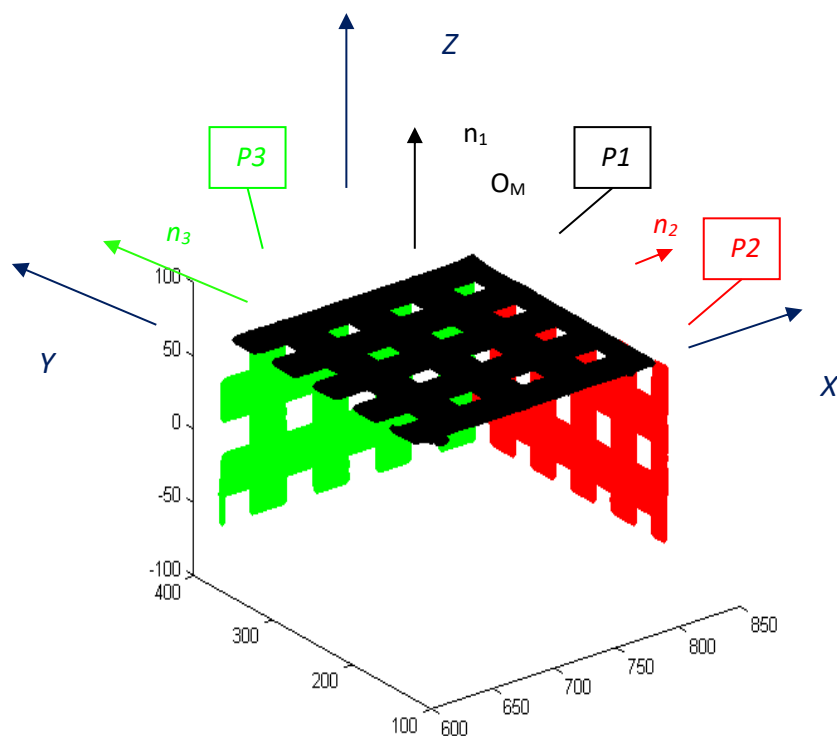


Figure 1. 3D calibration pattern for Points cloud obtained with the 3D scanner.

3. Matching a CCD camera and a 3D laser sensor

We present in this paper a method for matching a CCD camera and a 3D laser sensor. As a first step, calibrate the devices located in the same space, due to the standard calibration techniques G. CLOUD.(1998). Secondly calculate the transition matrix of the camera and the transition matrix of the 3D sensor. Third step calculation of total transformation matrix M_t for combining the texture image obtained with the camera, and the surface obtained with the 3D scanner. This method is illustrated in Figure 2., where for each vertex V_i point cloud obtained with the scanner associating a pixel P_i of the image obtained with the camera.

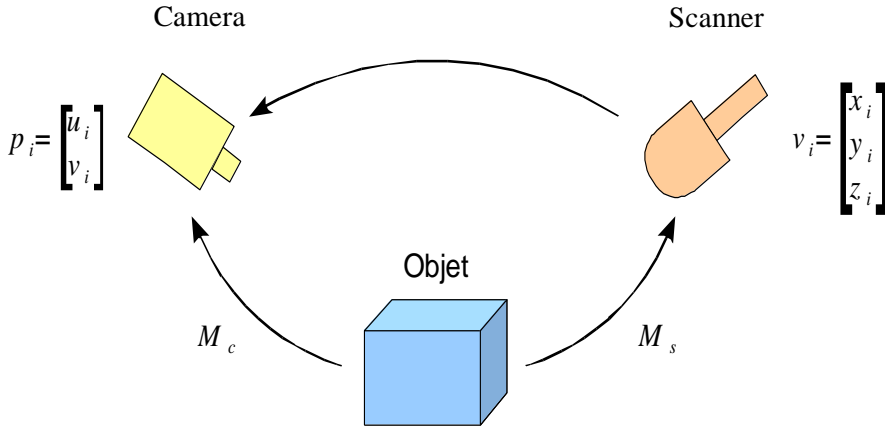


Figure 2. Coupling of the camera and the 3D laser scanner

4. Measuring Displacement

After calibration of the scanner and camera, we obtain an association between the pixel (u_i, v_i) of the camera image and the vertices (x_i, y_i, z_i) of the point cloud obtained with the scanner. At beginning, we acquire an object in an initial position, then move the object, and we repeat an acquisition. We select manually one specific characteristic point of the object to specify its characteristics before and after movement. In our experiment, the characteristic point is defined as a corner of a square of the calibration target.

We record the coordinates (u, v) of the characteristic point in each image and then compute the coordinates (x, y, z) from the top of the scanner. Finally, we measure the displacement as the Euclidean distance between the 3D point feature recorded before and after displacement:

$$D = \sqrt{(x_2 - x_1)^2 + (y_2 - y_1)^2 + (z_2 - z_1)^2} \quad (6)$$

$$D_x = x_2 - x_1, D_y = y_2 - y_1, D_z = z_2 - z_1 \quad (7)$$

where (x_1, y_1, z_1) and (x_2, y_2, z_2) are the coordinates of the characteristic point on the scatter plot before and after displacement .

5. Measuring Deformation

Mark and local deformations of rotations through a moving solid. We replace the object by its outer envelope will be considered without thickness.

The displacement is calculated by interpolation and are given in the reference measurement by a 3D vector field expressed in the reference measurement, $R(\vec{x}, \vec{y}, \vec{z})$:

$$\vec{U} \begin{bmatrix} u(x, y, z) \\ v(x, y, z) \\ w(x, y, z) \end{bmatrix}$$

purpose computing $\vec{\Omega} \begin{bmatrix} a \\ b \\ c \end{bmatrix}$ solid carrier rotation is

$$\omega = \begin{bmatrix} 0 & \frac{\partial u}{\partial y} - \frac{\partial v}{\partial x} & \frac{\partial u}{\partial z} - \frac{\partial w}{\partial x} \\ \frac{\partial v}{\partial x} - \frac{\partial u}{\partial y} & 0 & \frac{\partial v}{\partial z} - \frac{\partial w}{\partial y} \\ \frac{\partial w}{\partial x} - \frac{\partial u}{\partial z} & \frac{\partial w}{\partial y} - \frac{\partial v}{\partial z} & 0 \end{bmatrix} = \begin{bmatrix} 0 & -a & b \\ a & 0 & -c \\ -b & c & 0 \end{bmatrix} \quad (8)$$

It can be calculated from the tensor of local rotations

step 1: regular triangular mesh

Displacements are expressed as nodes attached to elements

Step2: calculating the shift with the actual element for reference (3D surface passing)

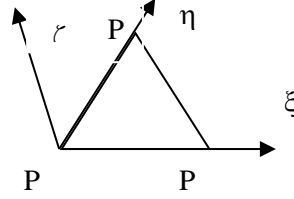
$$\vec{U} \begin{bmatrix} u(x, y, z) \\ v(x, y, z) \\ w(x, y, z) \end{bmatrix} \Rightarrow \vec{U}_e \begin{bmatrix} u_e(\xi, \eta) \\ v_e(\xi, \eta) \\ w_e(\xi, \eta) \end{bmatrix}$$

If the item is regular it can be considered as a reference only a scaling factor (divide by the area) and orientation will be different for each element is then calculated the change of reference to project item in the reference of the reference element

$$N_1=1-\xi-\eta; \quad \frac{\partial N_1}{\partial \xi} = \frac{\partial N_1}{\partial \eta} = -1; \quad \frac{\partial N_1}{\partial \zeta} = 0$$

$$N_2=\xi; \quad \frac{\partial N_2}{\partial \xi} = 1, \quad \frac{\partial N_2}{\partial \eta} = 0; \quad \frac{\partial N_2}{\partial \zeta} = 0$$

$$N_3=\eta; \quad \frac{\partial N_3}{\partial \xi} = 0, \quad \frac{\partial N_3}{\partial \eta} = 1; \quad \frac{\partial N_3}{\partial \zeta} = 0$$



$$\overrightarrow{P_i P_j} = \vec{\xi} = \frac{1}{[(x_j-x_i)^2+(y_j-y_i)^2+(z_j-z_i)^2]^{1/2}} \begin{bmatrix} x_j - x_i \\ y_j - y_i \\ z_j - z_i \end{bmatrix}, \quad \overrightarrow{P_i P_k} =$$

$$\vec{\eta} = \frac{1}{[(x_k-x_i)^2+(y_k-y_i)^2+(z_k-z_i)^2]^{1/2}} \begin{bmatrix} x_k - x_i \\ y_k - y_i \\ z_k - z_i \end{bmatrix}$$

$$\overrightarrow{P_i P_j} \wedge \overrightarrow{P_i P_k} = \vec{\zeta} \quad (9)$$

$$\overrightarrow{U_i} \cdot \vec{\xi} \Rightarrow u_{e1} = u_e(0,0); \quad \overrightarrow{U_i} \cdot \vec{\eta} \Rightarrow v_{e1} = v_e(0,0); \quad \overrightarrow{U_i} \cdot \vec{\zeta} \Rightarrow w_{e1} = w_e(0,0)$$

$$\overrightarrow{U_j} \cdot \vec{\xi} \Rightarrow u_{e2} = u_e(1,0); \quad \overrightarrow{U_j} \cdot \vec{\eta} \Rightarrow v_{e2} = v_e(1,0); \quad \overrightarrow{U_j} \cdot \vec{\zeta} \Rightarrow w_{e3} = w_e(1,0)$$

$$\overrightarrow{U_k} \cdot \vec{\xi} \Rightarrow u_{e3} = u_e(0,1); \quad \overrightarrow{U_k} \cdot \vec{\eta} \Rightarrow v_{e3} = v_e(0,1); \quad \overrightarrow{U_k} \cdot \vec{\zeta} \Rightarrow w_{e3} = w_e(0,1)$$

Step3 : calculation of strains in the coordinate system of the reference element

$\epsilon_{\xi\xi}, \epsilon_{\eta\eta}, \epsilon_{\xi\eta}$,

$$\mathbf{\epsilon}_{(\xi,\eta,\zeta)} = \begin{bmatrix} \epsilon_{\xi\xi} & \epsilon_{\xi\eta} & 0 \\ \epsilon_{\xi\eta} & \epsilon_{\eta\eta} & 0 \\ 0 & 0 & 0 \end{bmatrix} \quad (10)$$

Calculation with the assumption of small perturbations $\epsilon = 1/2[\nabla\vec{U} + \nabla\vec{U}^T]$

$$\epsilon_{\xi\xi} = \frac{\partial N_1}{\partial \xi} u_{e1} + \frac{\partial N_2}{\partial \xi} u_{e2} + \frac{\partial N_3}{\partial \xi} u_{e3} \quad (11)$$

$$\epsilon_{\eta\eta} = \frac{\partial N_1}{\partial \eta} v_{e1} + \frac{\partial N_2}{\partial \eta} v_{e2} + \frac{\partial N_3}{\partial \eta} v_{e3} \quad (12)$$

$$\epsilon_{\xi\eta} = \frac{1}{2} \left[\frac{\partial N_1}{\partial \eta} u_{e1} + \frac{\partial N_2}{\partial \eta} u_{e2} + \frac{\partial N_3}{\partial \eta} u_{e3} + \frac{\partial N_1}{\partial \xi} v_{e1} + \frac{\partial N_2}{\partial \xi} v_{e2} + \frac{\partial N_3}{\partial \xi} v_{e3} \right] \quad (13)$$

It is better to calculate the large deformation $\epsilon = 1/2[\nabla\vec{U} + \nabla\vec{U}^T + \nabla\vec{U} \cdot \nabla\vec{U}^T]$

Then

$$\epsilon_{\xi\xi} = \frac{\partial N_1}{\partial \xi} u_{e1} + \frac{\partial N_2}{\partial \xi} u_{e2} + \frac{\partial N_3}{\partial \xi} u_{e3} + \frac{1}{2} \left[\left[\frac{\partial N_1}{\partial \xi} u_{e1} + \frac{\partial N_2}{\partial \xi} u_{e2} + \frac{\partial N_3}{\partial \xi} u_{e3} \right]^2 + \left[\frac{\partial N_1}{\partial \xi} v_{e1} + \frac{\partial N_2}{\partial \xi} v_{e2} + \frac{\partial N_3}{\partial \xi} v_{e3} \right]^2 \right]$$

$$\epsilon_{\eta\eta} = \frac{\partial N_1}{\partial \eta} v_{e1} + \frac{\partial N_2}{\partial \eta} v_{e2} + \frac{\partial N_3}{\partial \eta} v_{e3} + \frac{1}{2} \left[\left[\frac{\partial N_1}{\partial \eta} u_{e1} + \frac{\partial N_2}{\partial \eta} u_{e2} + \frac{\partial N_3}{\partial \eta} u_{e3} \right]^2 + \left[\frac{\partial N_1}{\partial \eta} v_{e1} + \frac{\partial N_2}{\partial \eta} v_{e2} + \frac{\partial N_3}{\partial \eta} v_{e3} \right]^2 \right]$$

$$\begin{aligned} \epsilon_{\xi\eta} = & + \frac{1}{2} \left[\frac{\partial N_1}{\partial \eta} u_{e1} + \frac{\partial N_2}{\partial \eta} u_{e2} + \frac{\partial N_3}{\partial \eta} u_{e3} + \frac{\partial N_1}{\partial \xi} v_{e1} + \frac{\partial N_2}{\partial \xi} v_{e2} + \frac{\partial N_3}{\partial \xi} v_{e3} + \right. \\ & \left. \left[\frac{\partial N_1}{\partial \xi} u_{e1} + \frac{\partial N_2}{\partial \xi} u_{e2} + \frac{\partial N_3}{\partial \xi} u_{e3} \right] \left[\frac{\partial N_1}{\partial \eta} u_{e1} + \frac{\partial N_2}{\partial \eta} u_{e2} + \frac{\partial N_3}{\partial \eta} u_{e3} \right] + \left[\frac{\partial N_1}{\partial \xi} v_{e1} + \frac{\partial N_2}{\partial \xi} v_{e2} + \right. \right. \\ & \left. \left. \frac{\partial N_3}{\partial \xi} v_{e3} \right] \left[\frac{\partial N_1}{\partial \eta} v_{e1} + \frac{\partial N_2}{\partial \eta} v_{e2} + \right. \right. \\ & \left. \left. \frac{\partial N_3}{\partial \eta} v_{e3} \right] \right] \quad (16) \end{aligned}$$

Step 4: calculation of the tensor rotations ω and vector rotation $\vec{\Omega}$ in the coordinate system of the reference element

$$\vec{\Omega} \begin{bmatrix} a \\ b \\ c \end{bmatrix} \text{ et } \mathbf{\Omega}_{(\xi, \eta, \zeta)} = \begin{bmatrix} 0 & \gamma_{\xi\eta} & -\gamma_{\xi\zeta} \\ -\gamma_{\xi\eta} & 0 & \gamma_{\eta\zeta} \\ \gamma_{\xi\zeta} & -\gamma_{\eta\zeta} & 0 \end{bmatrix} \quad (17)$$

$$\gamma_{\xi\eta} = a_e = \frac{1}{2} \left[\left[\frac{\partial N_1}{\partial \eta} u_{e1} + \frac{\partial N_2}{\partial \eta} u_{e2} + \frac{\partial N_3}{\partial \eta} u_{e3} \right] - \left[\frac{\partial N_1}{\partial \xi} v_{e1} + \frac{\partial N_2}{\partial \xi} v_{e2} + \frac{\partial N_3}{\partial \xi} v_{e3} \right] \right] \quad (18)$$

$$\gamma_{\xi\zeta} = b_e = \frac{1}{2} \left[\left[\frac{\partial N_1}{\partial \xi} w_{e1} + \frac{\partial N_2}{\partial \xi} w_{e2} + \frac{\partial N_3}{\partial \xi} w_{e3} \right] \right] \quad (19)$$

$$\gamma_{\eta\zeta} = c_e = \frac{1}{2} \left[- \left[\frac{\partial N_1}{\partial \eta} w_{e1} + \frac{\partial N_2}{\partial \eta} w_{e2} + \frac{\partial N_3}{\partial \eta} w_{e3} \right] \right] \quad (20)$$

Step 5: calculation of deformations and rotations in the measurement space, $R(\vec{x}, \vec{y}, \vec{z})$:

The matrix P is defined by the vectors of the coordinate system of the element

$$\mathbf{\Pi} = [\vec{\xi}, \vec{\eta}, \vec{\zeta}]$$

Then

$$\mathbf{\mathcal{E}}_{(x,y,z)} = \mathbf{P}^T \mathbf{\mathcal{E}}_{(\xi, \eta, \zeta)} \mathbf{P} \quad (21)$$

6. Results

In our experiment, we acquired with the 3D scanner and CCD camera of our calibration pattern in an initial position. Then we moved precisely the pattern along the x axis, and makes a new acquisition. The displacement is measured in an area defined manually using the method given in the previous section.

The following tables gives the results in terms of Euclidean distance and Dx: X-axis component of MMT , Dy: Y-axis component of the MMT, Dz: Z-axis component of the MMT calculated for each point associated with a pixel and the standard deviations obtained for each template 1, 2 and 3.

Table1. The results of the displacements.

(a) : Euclidean distances (D)

No	1	2	3	4	5	Standard Deviation
D _{imagette1}	10.027	10.01	10.00	9.9901	9.980	0.0240
D _{imagette2}	10.009	9.971	9.99	10.001	10.003	0.0269
D _{imagette3}	9.997	9.964	9.99	9.987	9.999	0.0279

(b) : X-axis component of MMT (Dx)

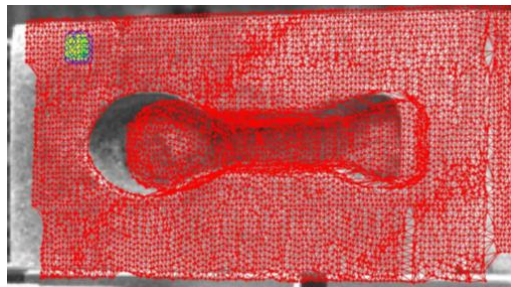
No	1	2	3	4	5	Standard Deviation
Dx _{imagette1}	-10.02	-10.009	-10.02	-9.99	-9.98	0.0234
Dx _{imagette2}	-10.00	-9.97	-9.98	-9.99	-10.00	0.0266
Dx _{imagette3}	-9.99	-9.98	-9.97	-9.98	9.97	0.0238

(c): Y-axis component of the MMT(Dy)

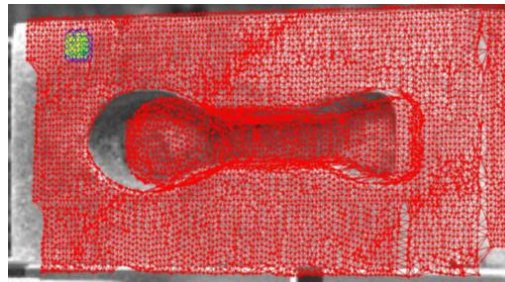
No	1	2	3	4	5	Standard Deviation
Dy _{imagette1}	-0.256	-0.246	-0.234	-0.217	-0.201	0.021
Dy _{imagette2}	-0.151	-0.122	-0.123	-0.136	-0.165	0.0229
Dy _{imagette3}	-0.116	-0.008	-0.009	-0.0087	0.0093	0.0238

(d) : Y-axis component of the MMT (Dz)

No	1	2	3	4	5	Standard Deviation
Dz _{imagette1}	-0.253	0.250	0.246	0.243	0.239	0.0082
Dz _{imagette2}	0.0048	-0.0051	-0.0054	-0.0056	-0.0062	0.0082
Dz _{imagette3}	0.0088	0.0084	0.0082	0.0079	0.0076	0.0083



template 1

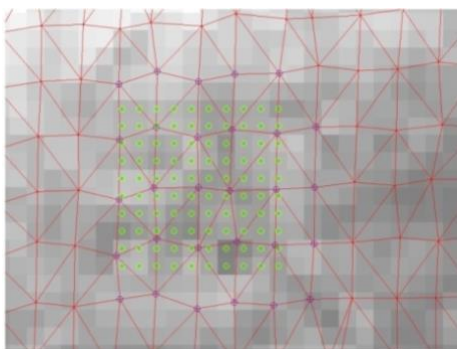


template 2

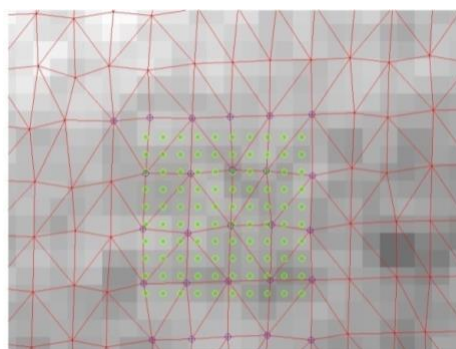


template 3

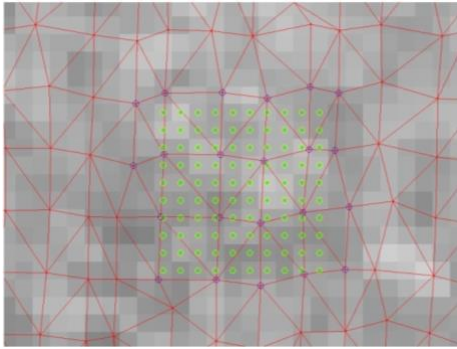
Figure 3. The study area of the selected templates.



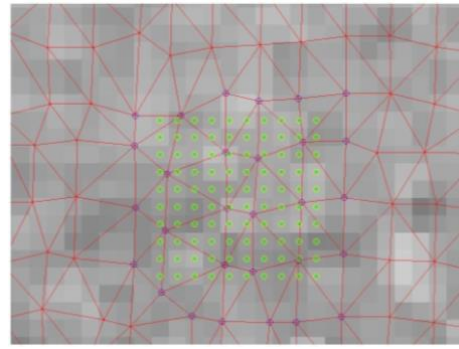
(a) template 1 before moving



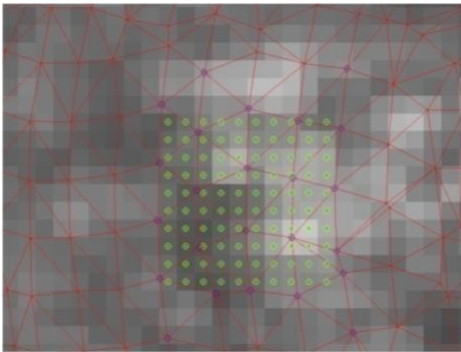
(b) template 1 after moving



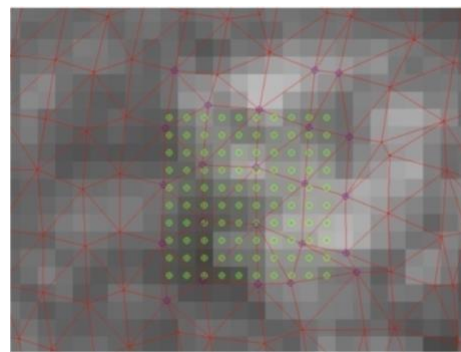
(a) template 2 before moving



(b) template 2 after moving



(a) template 3 before moving



(b) template 3 after moving

Figure 4. Reason associated with the templates 1,2,3

We note that for the measured displacement is close to the specified motion, the standard deviations for each measurement or for a pattern of 100 in the directions X and Y are of the order of 0.02 mm and the Z-direction of about 0.01 mm. On a practical level, the movement being in a plane containing the optical axis and in a direction approximately equal to 45° with respect thereto. It is logical that the dispersion along the Z axis which is parallel to the image plane is smaller. We also note that the results for 2 and 3 template, referring to surface and the other surface slightly left, are similar. Against the differences between the results of these templates and template 1 may be explained by calibration errors. The use of a non-linear calibration matrix would correct errors due to optical distortions and significantly improve the result.

6.1. Results of Measuring Deformation

Table2. The results of the deformation.

	$\varepsilon_1(\xi,\eta,\zeta)$	$\varepsilon_2(\xi,\eta,\zeta)$	$\varepsilon(\xi,\eta,\zeta)$
Zone1	$\begin{bmatrix} 0.0160 & 0.0243 & 0 \\ 0.0243 & 0.0329 & 0 \\ 0 & 0 & 0 \end{bmatrix}$	$\begin{bmatrix} 0.0242 & 0.0218 & 0 \\ 0.0218 & 0.0195 & 0 \\ 0 & 0 & 0 \end{bmatrix}$	
Zone2	$\begin{bmatrix} 0.0444 & -0.0305 & 0 \\ -0.0305 & 0.0182 & 0 \\ 0 & 0 & 0 \end{bmatrix}$	$\begin{bmatrix} 0.0030 & 0.0028 & 0 \\ 0.0028 & 0.0610 & 0 \\ 0 & 0 & 0 \end{bmatrix}$	
Zone3	$\begin{bmatrix} 0.0436 & -0.0278 & 0 \\ -0.0278 & 0.0138 & 0 \\ 0 & 0 & 0 \end{bmatrix}$	$\begin{bmatrix} 0.0115 & 0.0137 & 0 \\ 0.0137 & 0.0160 & 0 \\ 0 & 0 & 0 \end{bmatrix}$	

	$\bar{\Omega}_1$	$\bar{\Omega}_2$	$\bar{\Omega}$
Zone1	$\begin{bmatrix} 0.0084 \\ 0 \\ 0 \end{bmatrix}$	$\begin{bmatrix} -0.0024 \\ 0 \\ 0 \end{bmatrix}$	
Zone2	$\begin{bmatrix} 0.0127 \\ 1.1e-016 \\ 1.1e-016 \end{bmatrix}$	$\begin{bmatrix} 0.0025 \\ 0 \\ 0 \end{bmatrix}$	
Zone3	$\begin{bmatrix} 0.0144 \\ 0 \\ 0 \end{bmatrix}$	$\begin{bmatrix} 0.0022 \\ 2.7e-017 \\ 2.7e-017 \end{bmatrix}$	

	$\omega_1(\xi,\eta,\zeta)$	$\omega(\xi,\eta,\zeta)$
Zone1	$\begin{bmatrix} 0 & 0.0084 & 0 \\ -0.0084 & 0 & 0 \\ 0 & 0 & 0 \end{bmatrix}$	
Zone2	$\begin{bmatrix} 0 & 0.0127 & -1.1e-016 \\ -0.0127 & 0 & -1.1e-016 \\ 1.1e-016 & 1.1e-016 & 0 \end{bmatrix}$	
Zone3	$\begin{bmatrix} 0 & 0.0144 & 0 \\ -0.0144 & 0 & 0 \\ 0 & 0 & 0 \end{bmatrix}$	
	$\omega_2(\xi,\eta,\zeta)$	$\omega(\xi,\eta,\zeta)$
Zone1	$\begin{bmatrix} 0 & -0.0024 & 0 \\ -0.0024 & 0 & 0 \\ 0 & 0 & 0 \end{bmatrix}$	

Zone2	$\begin{bmatrix} 0 & 0.0025 & 0 \\ -0.0025 & 0 & 0 \\ 0 & 0 & 0 \end{bmatrix}$	
Zone3	$\begin{bmatrix} 0 & 0.0022 & -2.7e-017 \\ -0.0022 & 0 & -2.7e-017 \\ 2.7e-017 & 2.7e-017 & 0 \end{bmatrix}$	

	P1	P2	P3
Zone1	$\begin{bmatrix} -0.726 & -0.726 & 0.060 \\ -0.654 & -0.654 & -0.060 \\ 0.207 & 0.2079 & 0.0230 \end{bmatrix}$	$\begin{bmatrix} -0.727 & -0.727 & -0.014 \\ -0.6693 & -0.6693 & 0.0253 \\ 0.1486 & 0.1486 & 0.0433 \end{bmatrix}$	
Zone2	$\begin{bmatrix} -0.7594 & -0.7594 & -0.143 \\ -0.6480 & -0.6480 & 0.172 \\ 0.0582 & 0.0582 & 0.0574 \end{bmatrix}$	$\begin{bmatrix} -0.0709 & -0.0709 & 0.6508 \\ 0.0135 & 0.0135 & -0.7522 \\ 0.9974 & 0.9974 & 0.0564 \end{bmatrix}$	
Zone3	$\begin{bmatrix} -0.7499 & -0.7499 & -0.1656 \\ -0.6573 & -0.6573 & 0.1928 \\ 0.0743 & 0.0743 & 0.0342 \end{bmatrix}$	$\begin{bmatrix} 0.7342 & 0.7342 & -0.0329 \\ 0.6413 & 0.6413 & 0.0620 \\ 0.2229 & 0.2229 & -0.0700 \end{bmatrix}$	

	$\epsilon_{1(x,y,z)}$	$\epsilon_{2(x,y,z)}$	$\epsilon_{(x,y,z)}$
Zone1	$\begin{bmatrix} 0.0457 & 0.0457 & 0.00070 \\ 0.0457 & 0.0457 & 0.0007 \\ 0.0007 & 0.0007 & 5.64e-008 \end{bmatrix}$	$\begin{bmatrix} 0.0428 & 0.0428 & -0.0003 \\ 0.0428 & 0.0428 & -0.0003 \\ -0.0003 & -0.0003 & 0.000001 \end{bmatrix}$	
Zone2	$\begin{bmatrix} 0.0033 & 0.0033 & 0.0040 \\ 0.0033 & 0.0033 & 0.0040 \\ 0.0040 & 0.0040 & 0.0030 \end{bmatrix}$	$\begin{bmatrix} 0.00002 & 0.00002 & -0.0006 \\ 0.00002 & 0.00002 & -0.0006 \\ -0.0006 & -0.0006 & 0.0330 \end{bmatrix}$	
Zone3	$\begin{bmatrix} 0.0031 & 0.0031 & 0.0047 \\ 0.0031 & 0.0031 & 0.0047 \\ 0.0047 & 0.0047 & 0.0035 \end{bmatrix}$	$\begin{bmatrix} 0.0257 & 0.0257 & 0.0007 \\ 0.0257 & 0.0257 & 0.0007 \\ 0.0007 & 0.0007 & 1.8e-005 \end{bmatrix}$	

	$\omega_1(x,y,z)$	$\omega(x,y,z)$
Zone1	$\begin{bmatrix} 0 & 0 & 0.0007 \\ 0 & 0 & -0.0007 \\ -0.0007 & -0.0007 & 6.7e-021 \end{bmatrix}$	
Zone2	$\begin{bmatrix} 4.19e-019 & 4.19e-019 & -0.0029 \\ 4.19e-019 & 4.19e-019 & -0.0029 \\ 0.0029 & 0.0029 & 2.72e-020 \end{bmatrix}$	
Zone3	$\begin{bmatrix} -8.67e-019 & -8.67e-019 & -0.0037 \\ -8.67e-019 & -8.67e-019 & -0.0037 \\ 0.0037 & 0.0037 & 0 \end{bmatrix}$	
	$\omega_2(x,y,z)$	$\omega(x,y,z)$
Zone1	$\begin{bmatrix} 0 & 0 & 0.6673e-004 \\ 0 & 0 & 0.6673e-004 \\ -0.6673e-004 & -0.6673e-004 & 1.05e-022 \end{bmatrix}$	
Zone2	$\begin{bmatrix} -4.23e-022 & -4.23e-022 & 0.0001 \\ -4.23e-022 & -4.23e-022 & 0.0001 \\ 0.0001 & 0.0001 & 0 \end{bmatrix}$	
Zone3	$\begin{bmatrix} -5.34e-020 & -5.34e-020 & 0.000014 \\ -5.34e-020 & -5.34e-020 & 0.000014 \\ 0.000014 & 0.000014 & 5.79e-022 \end{bmatrix}$	

7. Conclusions

In this paper, we present a method for matching a CCD camera and a 3D laser sensor to obtain textured 3D model of an object observed. Then we proposed a method to calculate an estimate of the displacement using the point cloud and the image of the observed object present, we enhance this approach by automating the selection of areas measuring and controlling more finely calibration parameters. This work is part of an objective measurement of 3D deformation fields using the development tools.

References

- Cloud, G., (1998) Optical methods of engineering analysis, *Cambridge University Press*.
- Faugeras, O.D. and Toscani, G. (1986) "The calibration problem for stereo". *In Proc. Computer Vision and Pattern Recognition, Miami Beach, Florida, USA, 15-20*.
- Faugeras, O. D., Toscani, G.,(1987) Camera calibration for 3-D computer vision, Proceedings of IEEE International Workshop on Machine Vision years, *Machine Intelligence, Tokyo, Japan*.

Frey, P.J. and George, P.L. (1999) Meshes: application to finite elements, *Hermes Science Publication*.

Garcia, D. (2001) Measuring shape and displacement fields dimensional stereo-image correlation, *Ph.D. Thesis, Institut National Polytechnique de Toulouse, France*.

Garcia, D., Orteu, J.J. and Devy, M. (2000) Accurate Calibration of a Stereovision Sensor: Comparison of Different Approaches, *5th Visoin Workshop on Modeling, and Visualizaiton, Saarbrücken, Germany*.

Garcia, D., Orteu, J.J. and Devy, M. (2001) Precise calibration of a CCD camera or a stereoscopic vision sensor, *LAAS Report No. 01332 Photomécanique Symposium, Poitiers, France*.

Horaud, R. and Monga, O., (1995) Computer Vision: basic tools, 2nd edition.

Kinsey, L.C. (1993) Topology of Surfaces, *Springer-Verlag*.

Sutton, M.A., Wolters, W.J., Peters, W.H., Ranson, W.F. and McNeill, S.R. (1983) Determination of displacements using digital correlation An improved method. *Image and Vision Computing*, 1, (3), 133-139.

Sutton, M.A. (1988) The effects of subpixel picture restoration on digital correlation error estimates, 27, (3), 173-175.

Sutton, M.A., Cheng, M., Peters, W.H. Chao, Y.J. and McNeill, S.R., (1986) Application of optimized digital correlation method year to planar deformation analysis. *Image and Vision Computing*, 4, (3), 143-150.